Interplay between a phase response curve and spike-timing-dependent plasticity leading to wireless clustering

Hideyuki Câteau,[1,*] Katsunori Kitano,[2] and Tomoki Fukai[1,3]
[1]*Laboratory for Neural Circut Theory, RIKEN Brain Science Institute, 2–1 Hirowasa, Wako, Saitama 351-0198, Japan*
[2]*Department of Human and Computer Intelligence, Ritsumeikan University, 1-1-1 Nojihigashi, Kusatsu, Shiga 525-8577, Japan*
[3]*Department of Complexity Science and Engineering, University of Tokyo, Kashiwa, Chiba 277–8561, Japan*
(Received 28 March 2008; published 13 May 2008)

A phase response curve (PRC) characterizes the signal transduction between oscillators such as neurons on a fixed network in a minimal manner, while spike-timing-dependent plasiticity (STDP) characterizes the way of rewiring networks in an activity-dependent manner. This paper demonstrates that these two key properties both related to the interaction times of oscillators work synergetically to carve functionally useful circuits. STDP working on neurons that prefer asynchrony converts the initial asynchronous firing to clustered firing with synchrony within a cluster. They get synchronized within a cluster despite their preference to asynchrony because STDP selectively disrupts intracluster connections, which we call wireless clustering. Our PRC analysis reveals a triad mechanism: the network structure affects how the PRC is read out to determine the synchrony tendency, the synchrony tendency affects how the STDP works, and STDP affects the network structure, closing the loop.

DOI: 10.1103/PhysRevE.77.051909 PACS number(s): 87.19.L−, 87.18.Sn, 05.10.Gg, 02.50.Ey

Synchrony of a population of nonlinear oscillators has been a subject of interest in various biological systems as well as in physics [1–3]. Synchrony tendency of coupled oscillators or neurons is predicted by the phase response curve (PRC) of a neuron that describes an amount of advance or delay by synaptic input given at a specific phase in an interspike interval [1–4]. It is intriguing to know how this useful theory based on the fixed coupling strength between neurons generalizes to the cases where synaptic strength varies as observed in the real brain.

A number of experiments [5–10] have established that synaptic strength changes depending on presynaptic and postsynaptic spike times and theoretical implications of such spike-timing-dependent plasticity (STDP) have been extensively studied [11–19]. Since the PRC and STDP both refer to the timings of spikes, a natural question is how these two properties of a neuronal network interact with each other to carve a functional network in the brain.

To answer this question, we first use a neuron model whose PRC can be systematically controlled [20,21] unlike the simpler leaky integrate-and-fire (LIF) model. The model neurons favor either asynchronous (model A) or synchronous (model B) firing depending on the values of the model parameters.

Our simulations show that STDP working on the network of model A neurons converts asynchronously firing neurons into three or more cyclically activated clusters of neurons. Interestingly, model A neurons can synchronize within a cluster despite their preference to asynchrony because, as we see later, STDP selectively disrupts intracluster connections, nullifying the asynchrony preference.

When STDP works on the network of model B neurons, however, the neurons simply get synchronized globally, analogous to what was observed in Ref. [22], and nothing peculiar happens.

We will further show that the self-organized cyclic activity appears also under biologically realistic settings using a Hodgkin-Huxley-type neuron model, suggesting the generality of the concept.

In the self-organization, PRC specifies the timing preference and influences the way STDP works. Importantly, STDP in turn influences the way PRC is read out. Before the STDP learning begins, the initial slope of an effective PRC (defined later) determines the stability of the global synchrony. After the STDP learning forms the cyclic activity consisting of n clusters, the slope of the effective PRC at $\theta = 2\pi(1-1/n)$ determines its stability. In this way, the two key features of spiking neurons, PRC and STDP, work synergetically to organize functional networks in the brain.

STDP was previously shown [23–25] to help the pacemaker neuron entrain an innervated neuron(s), which was called "frequency synchrony" meaning that neurons start firing at the same frequency but with different phases as opposed to the "phase synchrony" studied here. Studying the frequency synchrony is the indispensable first step to understanding the oscillators or neurons because the phase synchrony is possible only after frequency synchrony is established. Building upon the firm theoretical ground of frequency synchrony [1,23–25], it is now important to ask when and how the frequency synchrony specializes to the phase synchrony because neurons in the phase synchrony can send out a large composite excitatory postsynaptic current (EPSC) that evokes a response in innervated neurons quite reliably. On the other hand, neurons in the frequency synchrony can only send out original tiny EPSC.

We consider a population of neurons firing quasiperiodically. To simulate the activity of the neurons, we use a spiking neuron model proposed by Izhikevich [20]. Depending

*Present address: Recognition and Judgement Unit, RIKEN BSI-Toyota Collaboration Center (BTCC), 2–1 Hirowasa, Wako, Saitama 351-0198, Japan

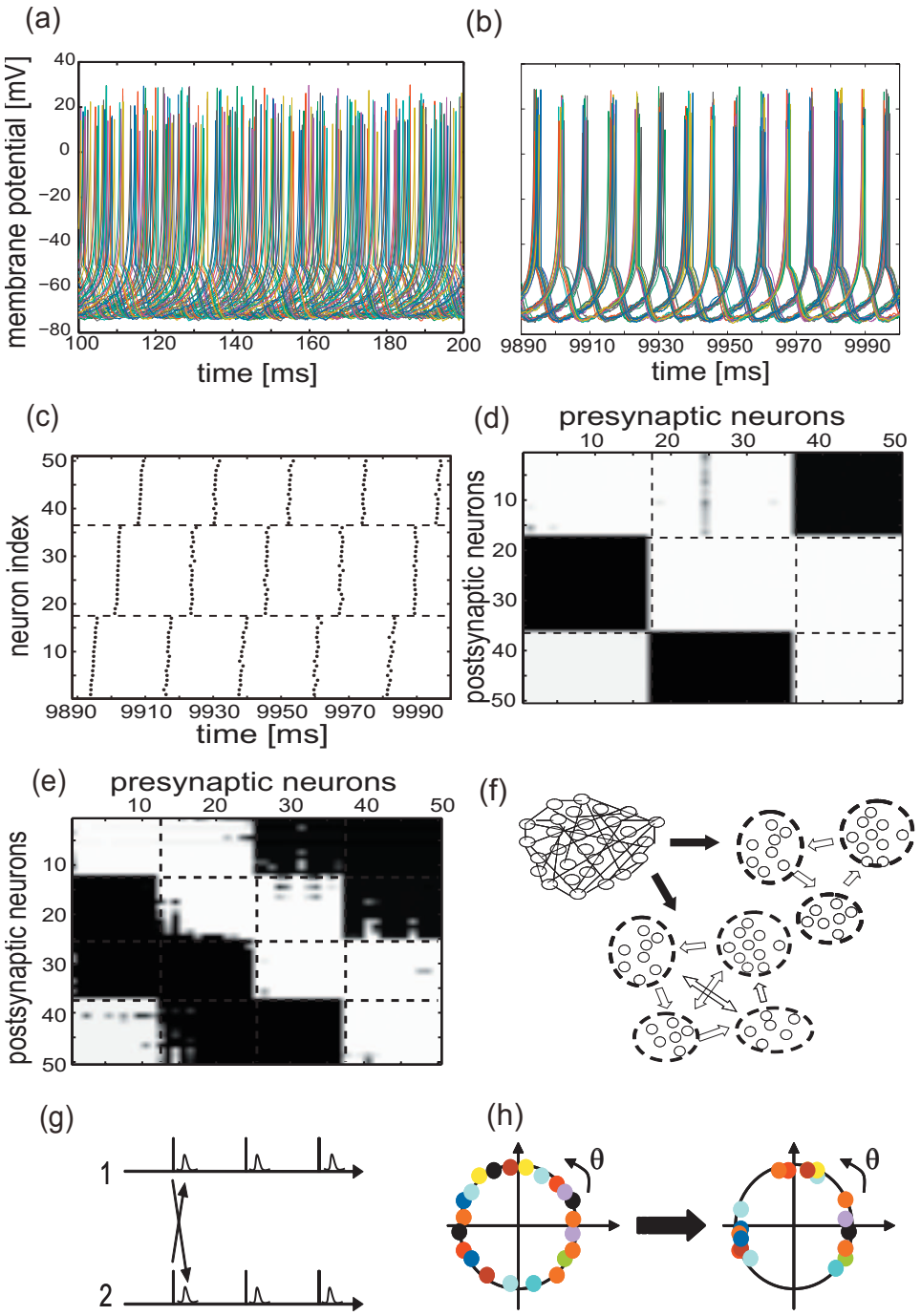

FIG. 1. (Color) Self-organized clustering of model A neurons by STDP. Fifty model A neurons fire in complete asynchrony before the STDP learning starts. (a) Voltage trajectories of all the neurons drawn in different colors are overlaid. (b) The neurons start firing in three different clusters with intracluster synchrony due to STDP. (c) A raster plot corresponding to (b). Neurons are aligned according to spike times. (d) A gray scale representation of the connection strength between neurons with black being the strongest. (e) The connection matrix when the higher-order rule of STDP is applied. A synaptic change is discounted by $1-\exp[-(t_{\text{postspike 2}}-t_{\text{EPSP by pre}})/\tau_{\text{remove}}]$ when a triplet of event, $t_{\text{postspike 1}}<t_{\text{EPSP by pre}}<t_{\text{postspike 2}}$, happened. (f) A schematic drawing showing the network topology corresponding to (d) and (e). [(g) and (h)] Positive feedback mechanism leading to the wireless clustering. In (g), the vertical lines indicate spike times of two neurons; the small wedges indicate EPSPs elicited by the spikes. In (h), distributed firing phases of neurons are represented by the filled circles in different colors.

on the values of four parameters, a, b, c, and d, this model can produce many different voltage trajectories similar to what are found in real neurons. Fifty model A neurons that favor asynchrony $(a=0.02, b=0.2, c=-50, d=1.26)$ are connected in an all-to-all manner with uniform synaptic strength and with a range of synaptic delays of 2 ± 0.2 ms. The neurons fire quasiperiodically driven by suprathreshold stochastic inputs, $I=I_0+\sigma\zeta(t)$ with $I_0=30$ mV/ms and $\sigma=1.5$ mV/ms$^{1/2}$, where $\zeta(t)$ is the Gaussian white noise.

With no synaptic plasticity at work, initial uniform distribution of firing phases [Fig. 1(a)] remain asynchronous because the neurons favor asynchrony. However, the effects of the standard additive STDP rule with hard boundaries $(0<w<1)$ defined [14] by

$$\Delta w=\begin{cases}A_+\exp(-\Delta t/\tau_+) & \text{for } \Delta t\geq 0\\ -A_-\exp(-|\Delta t|/\tau_-) & \text{for } \Delta t<0,\end{cases} \tag{1}$$

with $A_+=0.05$, $A_-=0.0525$ and $\tau_+=\tau_-=20$ ms converts the asynchronous firing into clusters of synchronous firing [Fig. 1(b)]. We note that there are cases where neurons neither favor the total synchrony nor the total asynchrony but are clustered due to higher harmonic components of a phase response curve without any involvement of the synaptic plasticity [26]. However, the phase response curve of the present model does not contain a large higher order harmonics and our simulations show no sign of clustering without the synaptic plasticity.

The network topology underlying this clustered synchronous firing is known by looking at the learned synaptic strengths as shown in Fig. 1(d), where neurons are indexed according to firing times after the learning ($t>9.89$ s). The firing interval is about 22 ms, so the synaptic delay is about 10% of it [27]. The three divisions apparent in Fig. 1(d) correspond to three synchronously firing clusters of neurons [Fig. 1(c)].

Interestingly, STDP turns out to have removed the intracluster connections almost completely [Fig. 1(d)]. In fact, such clustering without connections is observed commonly under various simulation conditions and we will call it wireless clustering.

To understand how it happens, we need to revisit the experimental literature of STDP with care. The standard STDP rule implies potentiation for positive timing difference $\Delta t = t_{\text{post}} - t_{\text{pre}} > 0$, and depression for a negative timing difference $\Delta t < 0$. Many have argued that the asymmetry of this rule produces a one-way coupling (see, e.g., Ref. [14]). Such arguments would be valid if $\Delta t = t_{\text{post}} - t_{\text{pre}}$ represented the time difference between postsynaptic and presynaptic spikes. However, actually most experimental literature [5–10] defines Δt to be the time difference between a postsynaptic spike and the onset or peak of the somatic excitatory postsynaptic potential (EPSP) induced by a presynaptic spike: $\Delta t = t_{\text{postspike}} - t_{\text{EPSP by pre}}$. Hence the above argument does not apply. A somatic EPSP should always lag behind a presynaptic spike for a few milliseconds. Therefore, if two neurons fire in exact synchrony [Fig. 1(g)], Δt is negative [23] for both directions, thereby weakens connections bidirectionally.

Now, how does this mechanism convert initial asynchronous firing to clustered synchronous firing [Fig. 1(b)]? Initial asynchronous firing [Fig. 1(a)] is represented as firing phases evenly spread around the circle [Fig. 1(h), left]. The firing remains asynchronous without STDP because the neurons favor asynchrony. However, with the phases of many neurons squeezed into the circle, any single neuron must have neighboring neurons that unwillingly fire synchronously with it [Fig. 1(h)]. Among these neurons, the above-mentioned mechanism weakens their connections bidirectionally. As their synaptic connections weaken, mutual repulsion is also weakened. This then further synchronizes their firings. This positive feedback mechanism develops wireless clusters naturally [Figs. 1(h)]. Although this mechanism qualitatively explains how the clustering happens, a quantitative question of how many clusters are formed requires further consideration. We will later see that a stability analysis tells the possible number of clusters.

In contrast to the vanishing intracluster connections, the intercluster connections survive and can be unidirectional [Fig. 1(d)], which defines the cyclic network topology such as shown in Fig. 1(f) (upper).

It is intriguing to ask how we can change this three-cycle topology. There are reports of higher-order rule of STDP [28,29] and such higher-order effects were systematically described by the formalism given in Ref. [30]. Here, we chose the rule proposed in [29] and find that it increases the number of clusters [Fig. 1(e)]. The higher-order rule implies the gross increase in the long-term potentiation (LTP) effect because LTP override the immediately preceding long-term depression (LTD), while LTP only partly cancels the immediately preceding LTD. The enhanced LTP effect is likely to increase the total number of potentiated synapses, which is consistent with the increased ratio of black areas in Fig. 1(e) compared to Fig. 1(d).

In contrast to such cluster-wise synchrony observed with model A neurons, model B neurons that favor synchrony ($a=0.02, b=0.2, c=-50, d=40$) self-organize into the globally synchronous state. Due to the global synchrony, mutual synaptic connections are largely lost, and each neuron ends up being driven by the external input individually, leaving little sense of being present as a population [27]. The global synchrony gives too strong an impact and also has minimal coding capacity because all the neurons behave in an identical manner, and it appears to bear more similarity to the pathological activity such as epileptic seizure in the brain than to meaningful information processing.

By contrast, the clustered synchrony arising in the network of model A neurons appears functionally useful. Generally in the brain, the unitary EPSP amplitude (~ 0.5 mV) is designed to be much smaller than the voltage rise needed to elicit firing (~ 15 mV). Therefore, single-neuron activity alone cannot cause other neurons to respond. Therefore, the single-neuron activity is unlikely to work as a carrier of information transferred back and forth in the brain. In contrast, the self-organized assembly of tens of model A neurons [Figs. 1(d)] looks to be an ideal carrier of information in the brain because their impact on other neurons is strong enough to elicit responses reliably. In addition, those clusters can code the timing.

The PRC, $Z(2\pi t/T)$, which represents the amount of advance or delay of the next firing time in response to the input at t in the firing interval $[0,T]$ has been mostly used to decide whether a coupled pair of neurons or oscillators tend to synchronize or desynchronize under the assumption that the connection strengths between the neurons are equal and unchanged. Specifically, when a pair of neurons are mutually connected and a spike of one neuron introduces a current with the wave form of EPSC(t) in an innervated neuron after a transmission delay of τ_d, the effective PRC defined as $\Gamma_-(\theta) = \frac{1}{T}\int_0^T Z(2\pi t'/T)\text{EPSC}(t' - \tau_d - T\frac{\theta}{2\pi})dt'$ decides their synchrony tendency. If the slope of $\Gamma_-(\theta)$ at $\theta=0$ is positive (negative), the two neurons are desynchronized (synchronized). This synchrony condition is considered to be taken over to a population of neurons coupled in an all-to-all or random manner as far as the connection strengths are unchanged. Theoretically calculated $\Gamma_-(\theta)$s for models A and B [Figs. 2(a) and 2(b)] explain that the nonplastic all-to-all network of model A (B) neurons exhibit global asynchrony (synchrony). Both model A and B neurons belong to type II [31] so that both model neurons favor synchrony if they are delta coupled with no synaptic delay. However, the biologically realistic couplings makes model A neurons favor asynchrony.

After STDP is switched on, the network consisting of model A neurons, is self-organized into the three-cycle circuit [Fig. 1(d)] with the successive phase difference of the clustered activity being equal to $\Delta_{\text{suc}}\theta = 2\pi/3$. We can show

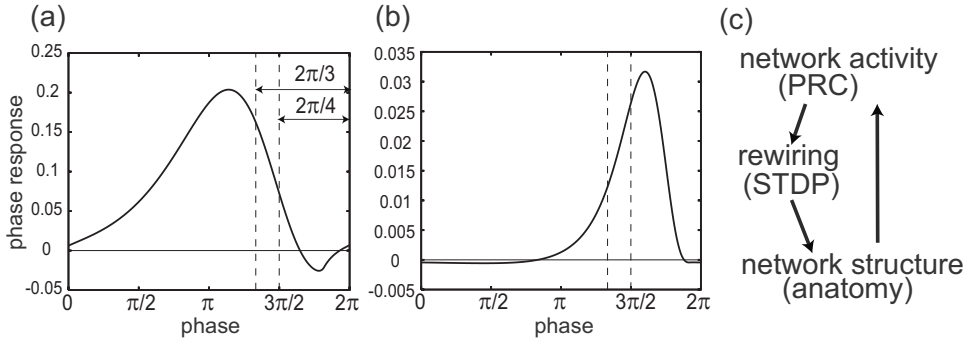

FIG. 2. Effective PRCs and a triad scheme. The effective PRC of models A and B are calculated with the adjoint method [21,31] and shown in (a) and (b). The slope at $\theta=0$ is positive for (a) but negative for (b) although it does not look clear with this resolution. The slope at $\theta=2\pi-2\pi/3$ is negative for (a) but positive for (b). The dashed lines represent $\theta=2\pi-2\pi/3$ and $\theta=2\pi-2\pi/4$. (c) The triad scheme by which PRC and STDP work synergetically to carve functional network.

that the slope of $\Gamma_-(\theta)$ not at the origin but at $\theta=2\pi-\Delta_{\mathrm{suc}}\theta$ now determines the stability of the three-cycle activity: if $\Gamma'_-(2\pi-\Delta_{\mathrm{suc}}\theta)<0$, the three-cycle activity is stable. Figure 2(a) ensures that the three-cycle activity shown in Fig. 1(c) is stable.

The stable state is achieved through the following synergetic process [Fig. 2(c)]: PRC determines the preferred network activity (e.g., asynchronous or synchronous), the network activity determines how STDP works, STDP modifies the network structure (e.g., from all-to-all to cyclic), and the network structure determines how the PRC is read out [e.g., $\theta=0$ or $\theta=2\pi-\Delta_{\mathrm{suc}}\theta$)], closing the loop.

Similarly, we can show that the n-cycle activity whose successive phase difference equals $\Delta_{\mathrm{suc}}\theta=2\pi/n$ is stable if $\Gamma'_-(2\pi-\Delta_{\mathrm{suc}}\theta)<0$. PRCs of biologically plausible neuron models or real neurons [32–41] generally have a negative slope in a later phase of the firing interval and converge to zero at $\theta=2\pi$ because the membrane potential starts the regenerative depolarization and becomes insensitive to any synaptic input. The corresponding effective PRCs inherit this negative slope in the later phase and tend to stabilize the n-cycle activity for some n.

Next we show that the self-organized cyclic activity in the wireless clustering is also observed in a biologically realistic setting. Our simulations as described in Ref. [42] with 200 excitatory and 50 inhibitory neurons modeled with the Hodgkin-Huxley (HH) formalism exhibit the three-cyclic activity with the wireless clustering [Figs. 3(a) and 3(b)], indeed. The firing interval is about 30 ms and the mean synaptic delay is about 4% of it. The setup here is biologically realistic in that (1) neurons are modeled with the HH formalism, (2) a physiologically known percentage of inhibitory neurons with nonplastic synapses are included, and (3) neurons fire with high irregularity due to large noise in the background input unlike the well-regulated firing as shown in Fig. 1(c).

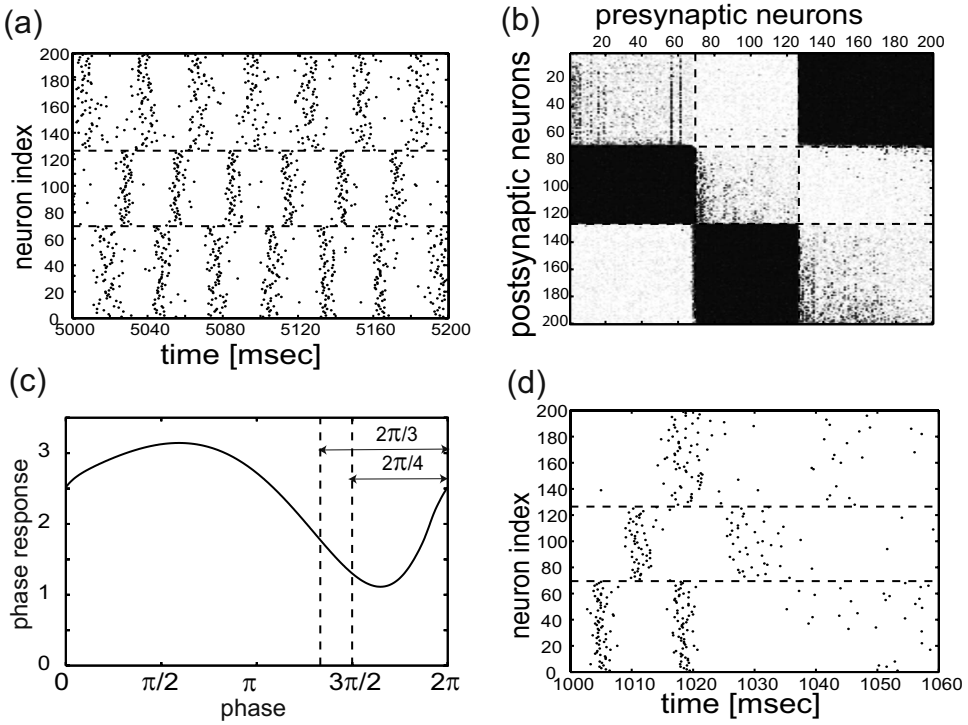

FIG. 3. Conductance-based model also develops the wireless clustering. (a) A raster plot of 200 HH-type excitatory neurons showing three-cycle activity. (b) The corresponding connection matrix showing the wirelessness. (c) Effective PRC or $\Gamma_-(\theta)$ of the conductance-based model. (d) The raster plot of the same neurons when the intracluster connections are set to exactly zero.

Interestingly, the effective PRC [Fig. 3(c)] of the HH-type neuron shares important features with that of model A: the positive initial slope implying the preference to asynchrony and a negative later slope stabilizing the three-cycle activity.

Technical difficulty in the HH simulations is, however, their massive computational demands due to the complexity of the system. That difficulty hindered theoretical analysis, therefore the study in Ref. [42] remained largely experimental. In particular, we tried hard to understand why we never observed four-cycle activity or longer, in vain. However, the analytic argument we developed here with the simplified model gives a clear insight into this complex system. A comparison of Figs. 2(a) and 3(c) reveals that the negative slope of $\Gamma_{-}(\theta)$ of the HH model is located more left than that of model A, indicating less stability of long cycles in the HH simulations. In addition, with the larger amount of noise in the HH simulations in mind, we can easily expect that four-cycle activity and longer can be destabilized in the HH simulations. Thus, the theory we developed here on the simplified system serves as a useful tool to understand complex systems.

Nevertheless, there is also an interesting difference between the model A and HH simulations. Apparently, the intracluster wirelessness is a fairly good approximation in the HH model simulations [Fig. 3(b)]. However, the wirelessness is not as exact as in the model A simulations [Figs. 1(d) and 1(e)]. Interestingly, an elimination of the residual intracluster connections destabilizes the cyclic activity [Fig. 3(d)], indicating the supportive role of the tiny residual intracluster connections.

In the previous simulation study Ref. [43] using the LIF model, cyclic activity was observed to propagate only at the theoretical speed limit: it takes only τ_d from one cluster to the next, implying the zero membrane integration time. To understand why it was the case, we first remind one that the effective PRC needs a negative slope at $2\pi-\Delta_{\mathrm{suc}}\theta$ to stabilize the cyclic activity. However, the slope of the original PRC of an LIF model, $Z(\theta)=c\exp(\frac{T}{\tau_m}\frac{\theta}{2\pi})$, is always positive except at the end point, where $Z(2\pi-0)=c\exp(\frac{T}{\tau_m})$ and $Z(2\pi+0)=c$, implying $Z'(2\pi)=-\infty$. This infinitely sharp negative slope of the PRC at $\theta=2\pi$ is rounded and displaced to $2\pi-2\pi\tau_d/T$ in the corresponding effective PRC, $\Gamma_{-}(\theta)$ (see its definition). Since this is the only point where $\Gamma_{-}(\theta)$ has a negative slope, the cyclic activity is stable only if $\Delta_{\mathrm{suc}}\theta=2\pi\tau_d/T$, implying the propagation at the theoretical speed limit.

We demonstrated an intimate interplay between PRC and STDP using the Izhikevich neuron model as well as the HH-type model. The self-organization or unsupervised learning by STDP studied here complements the supervised learning studied in [35]. The present study complements previous studies using the phase oscillator [22,25], where its mathematical tractability was exploited to analytically investigate the stability of the global phase or frequency synchrony. We derived a stability condition for the n-cycle activity. However, we note that this stability condition is a necessary condition but not a sufficient condition. In order to understand why the three-cycle activity preferentially appeared rather than the four-cycle, we may need more analytical studies. The propagation of synchronous firing and temporal evolution of synaptic strength under STDP is known to be analyzed semianalytically with the Fokker-Planck equation [15,16,18,19,44]. It is an interesting future direction to see how the Fokker-Planck equation can be used to understand the interplay between PRC and STDP.

Although STDP has been observed widely in the brain, what circuit can be formed by this plasticity remains elusive. The present study provides a clue to this question by demonstrating that the wireless clustering develops if STDP acts on a population of neurons working in the suprathreshold regime. We did not observe any nontrivial structure formation in the subthreshold regime. The decreasing firing regularity along the pathway from sensors to relay cells and to cortical cells [45] may imply that the wireless clustering applies better in the subcortical areas. In the rat visual cortex, they observed a cluster of excitatory neurons sharing the input [46]. However, their clusters were internally wired in contrast to what we saw here. Such wired, instead of wireless, clusters may be formed by a mechanism distinct from what we discussed here. Alternatively, wireless clusters might have been formed first under a suprathreshold condition in an early developmental stage, then additional plasticity has developed the intracluster coupling to reinforce the clusters. Exploring brain areas and states appropriate for the wireless clustering is the important future plan.

ACKNOWLEDGMENTS

The present authors thank Dr. T. Takekawa at RIKEN BSI for offering the code to calculate the PRC. They also thank Dr. J. Teramae at RIKEN BSI for critically reading the manuscript and for stimulating discussions. The present study was supported by Grants in Aid for Scientific Research of Priority Areas (Grant Nos. 17022036 and 18019036) from Japanese Ministry of Education, Culture, Sports, Science and Technology.

[1] Y. Kuramoto, *Chemical Oscillations, Waves, and Turbulence* (Springer-Verlag, Berlin, 1984).
[2] A. T. Winfree, J. Theor. Biol. **16**, 15 (1967).
[3] A. T. Winfree, *The Geometry of Biological Time* (Springer, New York, 1980).
[4] G. B. Ermentrout and N. Kopell, SIAM J. Math. Anal. **15**, 215 (1984).
[5] H. Markram *et al.*, Science **275**, 213 (1997).
[6] C. C. Bell *et al.*, Nature (London) **387**, 278 (1997).
[7] J. C. Magee and D. Johnston, Science **275**, 209 (1997).
[8] G. Q. Bi and M. M. Poo, J. Neurosci. **18**, 10464 (1998).
[9] D. E. Feldman, Neuron **27**, 45 (2000).

[10] M. Nishiyama *et al.*, Nature (London) **408**, 584 (2000).
[11] W. Gerstner *et al.*, Nature (London) **383**, 76 (1996).
[12] R. Kempter, W. Gerstner, and J. L. van Hemmen, Phys. Rev. E **59**, 4498 (1999).
[13] P. D. Roberts, J. Comput. Neurosci. **7**, 235 (1999).
[14] S. Song, K. D. Miller, and L. F. Abbott, Nat. Neurosci. **3**, 919 (2000).
[15] M. C. van Rossum, G. Q. Bi, and G. G. Turrigiano, J. Neurosci. **20**, 8812 (2000).
[16] J. Rubin, D. D. Lee, and H. Sompolinsky, Phys. Rev. Lett. **86**, 364 (2001).
[17] L. F. Abbott and S. B. Nelson, Nat. Neurosci. **3**, 1178 (2000).
[18] W. Gerstner and W. M. Kistler, *Spiking Neuron Model* (Cambridge University Press, Cambridge, 2002).
[19] H. Câteau and T. Fukai, Neural Comput. **15**, 597 (2003).
[20] E. M. Izhikevich, IEEE Trans. Neural Netw. **15**, 1063 (2004).
[21] T. Takekawa, T. Aoyagi, and T. Fukai, J. Comput. Neurosci. **23**, 189 (2007).
[22] J. Karbowski and G. B. Ermentrout, Phys. Rev. E **65**, 031902 (2002).
[23] T. Nowotny *et al.*, J. Neurosci. **23**, 9776 (2003).
[24] V. P. Zhigulin, M. I. Rabinovich, R. Huerta, and H. D. I. Abarbanel, Phys. Rev. E **67**, 021901 (2003).
[25] N. Masuda and H. Kori, J. Comput. Neurosci. **22**, 327 (2007).
[26] D. Golomb, D. Hansel, B. Shraiman, and H. Sompolinsky, Phys. Rev. A **45**, 3516 (1992).
[27] See EPAPS Document No. E-PLEEE8-77-078805 for simulation results with different values of the synaptic delay and input bias and results of simulations with model B. For more information on EPAPS, see http://www.aip.org/pubservs/epaps.html.
[28] R. C. Froemke and Y. Dan, Nature (London) **416**, 433 (2002).
[29] H. X. Wang *et al.*, Nat. Neurosci. **8**, 187 (2005).
[30] J. P. Pfister and W. Gerstner, J. Neurosci. **26**, 9673 (2006).
[31] B. Ermentrout, Neural Comput. **8**, 979 (1996).
[32] A. D. Reyes and E. E. Fetz, J. Neurophysiol. **69**, 1673 (1993).
[33] S. A. Oprisan, A. A. Prinz, and C. C. Canavier, Biophys. J. **87**, 2283 (2004).
[34] T. I. Netoff *et al.*, J. Neurophysiol. **93**, 1197 (2005).
[35] M. Lengyel *et al.*, Nat. Neurosci. **8**, 1677 (2005).
[36] R. F. Galan, G. B. Ermentrout, and N. N. Urban, Phys. Rev. Lett. **94**, 158101 (2005).
[37] A. J. Preyer and R. J. Butera, Phys. Rev. Lett. **95**, 138103 (2005).
[38] J. A. Goldberg, C. A. Deister, and C. J. Wilson, J. Neurophysiol. **97**, 208 (2007).
[39] T. Tateno and H. P. Robinson, Biophys. J. **92**, 683 (2007).
[40] J. G. Mancilla *et al.*, J. Neurosci. **27**, 2058 (2007).
[41] Y. Tsubo *et al.*, Eur. J. Neurosci. **25**, 3429 (2007).
[42] K. Kitano, H. Câteau, and T. Fukai, NeuroReport **13**, 795 (2002).
[43] N. Levy *et al.*, Neural Networks **14**, 815 (2001).
[44] H. Câteau and A. D. Reyes, Phys. Rev. Lett. **96**, 058101 (2006).
[45] P. Kara, P. Reinagel, and R.C. Reid, Neuron **27**, 635 (2000).
[46] Y. Yoshimura, J. L. Dantzker, and E. M. Callaway, Nature (London) **433**, 868 (2005).